Supporting information

The atomic-scale evolution of a growing core-shell nanoparticle

Shai Mangel[1], Eran Aronovitch[1], Andrey N. Enyashin[2], Lothar Houben[3], Maya Bar-Sadan[1]*

1 Department of Chemistry, Ben-Gurion University of the Negev, Beer-Sheva, Israel

2 Institute of Solid State Chemistry UB RAS, Ekaterinburg, Russian Federation

3 Peter Grünberg Institut 5 and Ernst Ruska-Centre for Microscopy and Spectroscopy with Electrons, Forschungszentrum Jülich GmbH, 52425 Jülich, Germany.

1. Experimental:

Materials:

The following materials were used: CdO (99.999%, Strem Chemicals, MA, USA),, Se (99.999%, Alfa-Aesar, MA, USA), trioctylphosphine (TOP; 97%, Sigma-Aldrich, Israel), trioctylphosphine oxide (TOPO; 99%, Sigma-Aldrich, Israel), octadecylphosphonic acid (ODPA; 99%, Polycarbon Industries, MA, USA), S (99.98%, Sigma-Aldrich, Israel), oleic acid (90%, Alfa-Aesar, MA, USA),1-Octadecene ODE (90%, Sigma-Aldrich, Israel), Octadecylamine ODA (90%, Sigma-Aldrich, Israel), hexane (90%, Bio-Lab, Israel), toluene (90%, Bio-Lab, Israel).

Synthesis of CdSe cores: We followed the procedure described by Amirav et al.[1]. CdO (0.06 g, 0.47 mmol), TOPO (3 g) and ODPA (0.313 g) were loaded into a 25 ml triple-necked flask and heated to 150°C. The system was maintained under N_2 for around 60 min to eliminate water residues and impurities, and it was then heated under a N_2 flow to 300°C. Once a clear solution was obtained, 1.8 ml of TOP were injected into the mixture, and the temperature was set to 360°C. Thereafter, a solution of 0.058 g Se (0.735 mmol) dissolved in 1 ml of TOP was swiftly injected to the flask. The temperature rapidly declined to 330°C, and the heating mantle was removed after 30 s.

Following the synthesis, particles were precipitated by adding methanol and isolated by centrifugation. The precipitated nanocrystals were washed by re-dissolution in toluene and precipitation in methanol. The final product was dissolved in toluene.

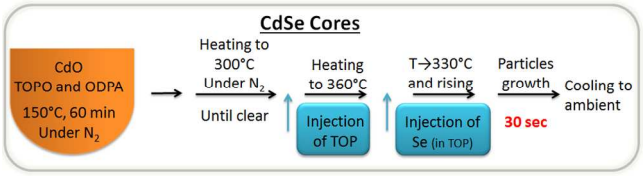

Figure S1. Summary of the synthetic procedure of the CdSe nanoparticles

Transfer of the CdSe cores to hexane: The toluene solvent of a solution containing $1.48 \cdot 10^{-4}$ mmol CdSe cores was completely evaporated by a Hei-VAP Value evaporator (Heidolph, Germany). The CdSe residue was suspended in 5.43 ml hexane (41.5 mmol).

***Synthesis of CdS shells*:** We used a modification of the procedure described by Blackman et al. [2]. The CdSe cores solution in hexane ($4.00 \cdot 10^{-5}$ mmol CdSe particles in 1.47 ml or 41.5 mmol hexane) was mixed with a mixture of ODA (0.604 g, 2.24 mmol) and ODE (2.55 ml, 8.00 mmol) in a 25 ml triple-necked flask. The system was pumped for around 60 min to eliminate water residues and impurities, and then again for 10 min at 100°C. Next, the system was heated to 190°C followed by injections of Cd^{2+} or S^{2-} solutions. The injection volume was adjusted to contain the number of atoms required to produce a single monolayer. Each subsequent injection should contain greater amounts of ions to cover completely the larger interface of the particle.

The Cd^{2+} solution was prepared as follows: CdO (0.040 g, 0.312 mmol) was dissolved in a mixture of oleic acid (0.786 ml, 2.49 mmol) and ODE (7.04 ml, 22.1 mmol) at 250°C in a 25-ml triple-necked flask. The final concentration of Cd^{2+} in the solution was 0.04 M. The S^{2-} solution was prepared as follows: elemental S (0.080 g, 0.312 mmol) was dissolved in ODE (7.80 ml, 24.50 mmol) at 200°C in a 25-ml triple-necked flask. The final concentration of S^{-2} in the solution was 0.04 M.

The Cd^{2+} solution was first injected into the cores solution, and the temperature was maintained at 190°C for 5 min. Then, the S^{2-} solution was injected, the temperature was set to 250°C, and the solution was stirred for 20 min. For the next cycle, the temperature was again decreased to 190°C, and the procedure was repeated to produce the desired number of layers in the shell. At the end of the process, the solution was allowed to cool to ambient temperature, transferred to a 125-ml separatory funnel, diluted with hexane, and extracted with methanol. The top hexane layer, which contained the particles, was transferred to a 15-ml centrifuge tube. The nanocrystals were precipitated by adding

methanol and isolated by centrifugation. The final product was dissolved in toluene.

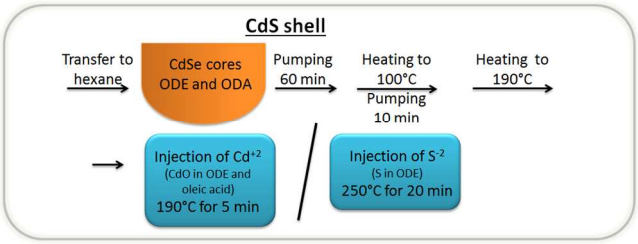

Figure S2. Summary of the synthetic procedure of the CdS shell.

***Preparation of TEM samples*:** The CdSe cores and the CdSe@CdS particles in toluene were precipitated with methanol and re-dissolved in toluene. Then, a drop of the solution was placed on graphene TEM grids (CVD graphene film on Lacy carbon 300 mesh, Graphene Supermarket, NY, USA) and left to evaporate. The dried grids were cleaned with a custom-made apparatus combining gentle heating (50°C) and vacuum (10^{-7} mbar) for 5 days under N_2 and kept in an inert atmosphere until mounting on the TEM.

TEM measurements were performed using the spherical and chromatic double aberration-corrected FEI 60-300 Ultimate [3] ('PICO') at the Ernst Ruska-Centre, Germany. TEM images were acquired at 80 kV acceleration voltage with a spherical aberration value of -5 µm and a chromatic aberration value smaller than 1 µm. Optimized phase contrast for TEM images was achieved at a slight overfocus of +5 nm with a point resolution better than 1.1 Å. Focal series reconstruction (FSR) was used to retrieve the phase of the electron exit plane wavefunction[4]. Experimental focal series were taken with an equidistant focal step of 1.5 nm, corresponding to about half the defocus spread of the microscope at the respective acceleration voltage. Twenty images were recorded around the negative spherical-aberration imaging (NCSI) defocus (+5 nm in the conditions mentioned above) for the phase retrieval using the Brite/Euram focal series reconstruction (FSR) algorithms based on maximum-likelihood algorithms for nonlinear reconstruction[4]. The reconstructed wavefunction was Fourier-filtered to subtract the graphene layers background. For the average size and aspect ratio, about 70 particles of each sample were analyzed.

***Preparation of XRD samples*:** The CdSe cores in toluene were precipitated in methanol and redissolved in 0.5 ml of hexane. The solution was dripped onto a small Si wafer, and the solvent was evaporated on a heating mantle. Data were collected on Panalytical Empyrean Powder Diffractometer equipped with position sensitive (PSD) X'Celerator detector using Cu K_α radiation (λ=1.5405 Å) and operated at 40 kV and 30 mA. The usual Bragg-Brentano $\theta/2\theta$ and grazing incident beam geometry were employed. The grazing incident scan was performed at a constant incident beam angle of 2° in a 2θ range of 20°-60° with a step of 0.05° and 2 s per step.

Optical measurements: A small amount (0.1 ml) of sample was taken from each batch and diluted with toluene to an optical density of 0.1- 0.2. UV absorption spectra were measured with a Shimadzu UV-3600 spectrophotometer. Photoluminescence (PL) emission spectra were measured with a Shimadzu spectrofluorophotometer RF-5301pc.

2. EFTEM measurements

The core-shell structure of the CdSe@CdS particles was verified by energy-filtered TEM (EFTEM). Atomic-resolution EFTEM images were recorded using the spherical and chromatic aberration-double corrected FEI Titan 60-300 Ultimate ('PICO') at the Ernst Ruska-Centre, Germany. The use of chromatic aberration-correction allowed spectroscopic energy-filtered imaging with atomic optical resolution[5] even at the low acceleration voltage of 80 kV. Element-specific images were obtained with a Quantum GIF electron spectrometer and imaging filter (Gatan) by selecting transmitted electrons that were inelastically scattered by excitation of bound electrons. The resulting 'core-loss' images are characteristic of the scattering element. A series of EFTEM images was taken in a range between 30 eV and 200 eV energy loss, with a 20 eV wide energy selecting slit. Element-specific images were obtained after sub-pixel alignment of the raw data followed by a pixel-wise background fit (using a many-window method) and a background subtraction. Elemental maps of phosphorous visualized the capping phosphoric ligands, selenium-selective images revealed a homogeneous core structure, and sulfur-to-selenium ratio maps uncovered the CdSe@CdS core-shell composition with a sulfur-rich shell of approximately 1 nm thickness (Figure S3).

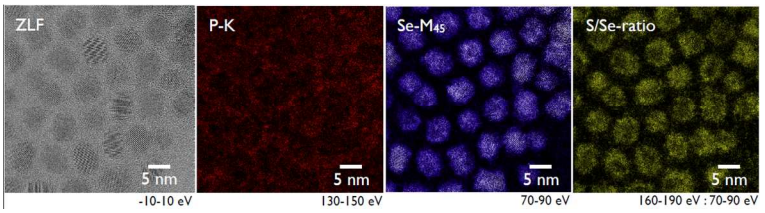

Figure S3. High-resolution EFTEM images of CdSe-CdS core-shell particles. From left to right: A zero-loss filtered (ZLF) image; background-corrected elemental maps of P and Se (P-K and SE-M_{45}, respectively); and a map of the elemental ratio between S and Se (S/Se-ratio). The elemental map of P, obtained from P K-shell core-loss excitations with the onset energy of 132 eV, shows termination by phosphoric ligands. The Se map recorded from Se M_{45}-shell excitations with the onset energy of 57 eV shows a mostly homogeneous core composition. The combined S and Se signal obtained from S K-shell excitation at 165 eV energy loss and weaker Se M_{23} shell excitation at 162 eV, plotted against the Se M_{45} signal, is used to display the presence and location of S. The bright concentric rings around the particles correspond to high sulfur content and disclose the core-shell structure with an approximately 1 nm thick sulfur-rich shell.

3. DFTB calculations

Density-functional based tight-binding (DFTB) calculations were performed using the SIESTA 2.0 implementation[6] within the framework of the density-functional theory (DFT)[7]. The exchange-correlation potential within the local-density approximation (LDA) with the Perdew-Zunger parameterization was used[8]. The core electrons were treated within the frozen core approximation, applying norm-conserving Troullier-Martins pseudopotentials[9]. The valence electrons were taken as $3s^2 3p^4$ for

S, as $4s^2 4p^4$ for Se, and as $5s^2 5p^2$ for Cd. Cd$4d^{10}$ electrons were included as a semi-core state. The pseudopotential core radii were chosen as suggested by Martins, and were equal to 1.70 a_B for all states of S, to 1.90 a_B for all states of Se, and to 2.65 a_B for all states of Cd. In all calculations, a double-ζ basis set was used for all atoms.

For *k*-point sampling, a cutoff of 10 Å was used[10]. The *k*-point mesh was generated by the method of Monkhorst and Pack[11]. The real-space grid used for the numeric integrations was set to correspond to an energy cutoff of 300 Ry. All calculations were performed using variable-cell and atomic position relaxation, with convergence criteria set to correspond to a maximum residual stress of 0.1 GPa for each component of the stress tensor, and a maximum residual force component of 0.01 eV/Å.

The test calculations were performed for examples of unit cells for the bulk hexagonal (wurtzite, w) and face-centered cubic (zinc blende, z) phases of both CdS and CdSe compounds. Models of interfaces are presented by the periodic supercells, which include two slabs and two equivalent interfaces. The supercells correspond to a 1×1×6 cell of w-CdS(Se) or a 1×1×4 cell of z-CdS(Se) in hexagonal representation, i.e., only interfaces related to wurtzite (001) or zinc blende (111) surfaces were considered. The resulting calculated lattice parameters and energies are shown in Table S1.

The calculations were performed for various combinations of the interface composition (w-CdS, z-CdS, w-CdSe, and z-CdSe) and interface boundaries (wurtzite-like or zinc blende-like). The estimated strain energy at the (001) interfaces of CdS|CdSe, independent of the phase state, was about 5 meV/Å^2. Thus, the experimentally observable difference in the phase composition at the CdS|CdSe interface cannot be explained by the strain. This conclusion was drawn in all the cases examined.

Table S1. Comparison of experimental and calculated (SIESTA) values for structural parameters of two modifications of CdS and CdSe compounds.

	Lattice parameters		Stability	
	Calc (Å)	Exp (Å)	Calculated E_{tot}	Experimental observation
w-CdS	a = 4.100 c = 6.700	a = 4.135 c = 6.749	-1485.6445 eV/ CdS	stable
z-CdS	a = 5.798	a = 5.820	-1485.6424 eV/ CdS	metastable
w-CdSe	a = 4.264 c = 6.967	a = 4.300 c = 7.020	-1465.3576 eV/ CdSe	stable
z-CdSe	a = 6.026	a = 6.080	-1465.3555 eV/ CdSe	metastable

Experimental values are taken from D.W. Palmer, www.semiconductors.co.uk, 2008.03.

References

1. Amirav, L.; Alivisatos, A. P., Photocatalytic Hydrogen Production with Tunable Nanorod Heterostructures. *The Journal of Physical Chemistry Letters* **2010,** *1* (7), 1051-1054.
2. Blackman, B.; Battaglia, D. M.; Mishima, T. D.; Johnson, M. B.; Peng, X., Control of the Morphology of Complex Semiconductor Nanocrystals with a Type II Heterojunction, Dots vs Peanuts, by Thermal Cycling. *Chemistry of Materials* **2007,** *19* (15), 3815-3821.
3. Haider, M.; Hartel, P.; Mueller, H.; Uhlemann, S.; Zach, J., Information Transfer in a TEM Corrected for Spherical and Chromatic Aberration. *Microscopy and Microanalysis* **2010,** *16* (4), 393-408.
4. (a) Coene, W. M. J.; Thust, A.; Op de Beeck, M.; Van Dyck, D., Maximum-likelihood method for focus-variation image reconstruction in high resolution transmission electron microscopy. *Ultramicroscopy* **1996,** *64* (1), 109-135; (b) Thust, A.; Coene, W. M. J.; Op de Beeck, M.; Van Dyck, D., Focal-series reconstruction in HRTEM: simulation studies on non-periodic objects. *Ultramicroscopy* **1996**.230-211 ,(1) 64 ,
5. (a) Urban, K. W.; Mayer, J.; Jinschek, J. R.; Neish, M. J.; Lugg, N. R.; Allen, L. J., Achromatic Elemental Mapping Beyond the Nanoscale in the Transmission Electron Microscope. *Physical Review Letters* **2013,** *110* (18), 185507; (b) Kabius, B.; Hartel, P.; Haider, M.; Müller, H.; Uhlemann, S.; Loebau, U.; Zach, J., First Application of Cc Corrected Imaging for High-Resolution and Energy-Filtered TEM. *Microscopy and Microanalysis* **2009,** *15* (SupplementS2), 1456-1457.
6. (a) Ordejón, P.; Artacho, E.; Soler, J. M., Self-consistent order-N density-functional calculations for very large systems. *Physical Review B* **1996,** *53* (16), R10441; (b) Soler, J. M.; Artacho, E.; Gale, J. D.; García, A.; Junquera, J.; Ordejón, P.; Sánchez-Portal, D., The SIESTA method for ab initio order-N materials simulation. *Journal of Physics: Condensed Matter* **2002,** *14* (11), 2745.
7. Hohenberg, P.; Kohn, W., Inhomogeneous Electron Gas. *Physical Review* **1964,** *136* (3B), B864-B871.
8. Perdew, J. P.; Zunger, A., Self-interaction correction to density-functional approximations for many-electron systems. *Physical Review B* **1981,** *23* (10), 5048-5079.
9. Troullier, N.; Martins, J. L., Efficient pseudopotentials for plane-wave calculations. *Physical Review B* **1991,** *43* (3), 1993-2006.
10. Moreno, J.; Soler, J. M., Optimal meshes for integrals in real- and reciprocal-space unit cells. *Physical Review B* **1992,** *45* (24), 13891-13898.
11. Monkhorst, H. J.; Pack, J. D., Special points for Brillouin-zone integrations. *Physical Review B* **1976,** *1*-5188 ,(12) 3 5192.